

Utilization of 3-D Imaging Flash Lidar Technology for Autonomous Safe Landing on Planetary Bodies

*Farzin Amzajerdian¹, Michael Vanek¹, Larry Petway¹, Diego Pierrotte², George Busch²,
Alexander Bulyshev³*

*1. NASA Langley Research Center, Hampton, Virginia 23681, USA
Tel.: 757-864-1533, Fax: 757-864-8828, E-mail: f.amzajerdian@nasa.gov*

2. Coherent Applications, Inc., Hampton, Virginia, USA

3. Analytical Mechanics Associates, Inc., Hampton, Virginia, USA

ABSTRACT

NASA considers Flash Lidar a critical technology for enabling autonomous safe landing of future large robotic and crewed vehicles on the surface of the Moon and Mars. Flash Lidar can generate 3-Dimensional images of the terrain to identify hazardous features such as craters, rocks, and steep slopes during the final stages of descent and landing. The onboard flight computer can use the 3-D map of terrain to guide the vehicle to a safe site.

The capabilities of Flash Lidar technology were evaluated through a series of static tests using a calibrated target and through dynamic tests aboard a helicopter and a fixed wing aircraft. The aircraft flight tests were performed over Moon-like terrain in the California and Nevada deserts. This paper briefly describes the Flash Lidar static and aircraft flight test results. These test results are analyzed against the landing application requirements to identify the areas of technology improvement. The ongoing technology advancement activities are then explained and their goals are described.

Key words: Flash Lidar, Ladar, 3-D Imaging, Laser Radar, Laser Remote Sensing, Landing Sensor

1. INTRODUCTION

The imaging Flash Lidar is being considered as the primary sensor, due to its ability to provide 3-Dimensional images of surfaces and hazards, for future robotic and manned landing missions to the Moon and Mars. An imaging lidar system records a three dimensional (3D) image of a scene by converting intensity versus time of flight of short laser pulses into intensity versus distance along the line of sight for each spatially resolved area within a 2D image. In older, more conventional imaging lidar systems, each 2D pixel is recorded with a separate laser pulse. Thus many laser pulses are required to record large, multi-pixel images. A Flash Lidar system records full 3D images with a single laser pulse, permitting higher data rates and freezing out movement within the scene and motion of the transmitter/receiver platform. The need for high speed raster scanners to sequentially address image pixels is also eliminated. The receiver is much like the familiar digital camera, but with "smart pixels" that are capable of recording the required sequential temporal information. NASA Langley Research Center (NASA-LaRC) has been assessing the potentials of Flash Lidar technology as a landing sensor and working on its advancement under the Autonomous Landing and Hazard Avoidance (ALHAT) project for the past 3 years. The ALHAT project, led by NASA Johnson Space Center, is established by NASA to develop and demonstrate a guidance, navigation, and control system for future lunar missions capable of terrain hazard avoidance and precision landing under any lighting conditions anywhere on the Moon¹.



Figure 1. Future lunar landing missions are considering scientifically interesting sites near craters and rough terrains.

To fulfill the requirements of global lunar access under any lighting conditions, ALHAT is pursuing active sensor technology development and maturation to implement five sensor functions: Altimetry, Velocimetry, Terrain Relative Navigation (TRN), Hazard Detection and Avoidance (HDA) and Hazard Relative Navigation (HRN). Table 1 below lists the ALHAT sensor suite and their top level performance specifications for achieving each of required functions with some degree of redundancy. Flash Lidar is being considered for performing all these functions with exception of velocimetry for which a Doppler Lidar is being developed. The ability of the Doppler Lidar to provide velocity data with approximately 1 cm/sec is highly attractive for precision landing. Additionally, the Doppler Lidar provides high resolution altitude and ground-relative attitude data that may further improve precision navigation to the identified landing site. Description of the Doppler lidar and its capabilities have been reported earlier^{2,3}. The Laser Altimeter provides independent altitude data over a large operational altitude range of 20 km to 100 m. All three laser sensors have a nominal update rate of 30 Hz.

Table 1. ALHAT Sensor Suite.

Sensor	Function	Operational Altitude Range	Precision/Resolution
Flash Lidar	HDA/HRN	1000 m – 100 m	5 cm/40 cm
	TRN	15 km – 5 km	20 cm/6 m
	Altimetry	20 km – 100 m	20 cm
Doppler Lidar	Velocimetry	2500 m – 10 m	1 cm/sec
	Altimetry	2500 m – 10 m	5 cm
Laser Altimeter	Altimetry	20 km – 100 m	20 cm

All five of the aforementioned functions provide input to the navigation filter for Landing Vehicle “state” estimation, flight trajectory retargeting, and maneuvering to a safe site. Of these five functions, Altimetry and Velocimetry are direct sensor measurements, whereas the TRN, HDA, and HRN functions can be considered relative measurements, since the sensor “output” is derived from a correlation with either “a priori” terrain information, or with a sequence of previous sensor measurements. The later functions can also be considered techniques, since a number of sensor – algorithm combinations can achieve similar results under the appropriate concept of operation. The location determination of safe landing sites is made from the location determination of hazards, simultaneously recorded within full 3-D images in complete spatial and temporal resolution. The simultaneity of the recording of full 3_D scenes with single laser pulses

not only enables more rapid acquisition, but simpler and more rapid processing of scene information to enable the time-sensitive precision navigation necessary to avoid hazards and land precisely at the retargeted location.

2. FLASH LIDAR OPERATIONAL CONCEPT

As noted above, the Flash Lidar serves as a multi-functional sensor capable of performing 4 out of 5 ALHAT functions. The current operational concept is based on a Flash Lidar system capable of generating 256x256 pixels image frames from a nominally 1 km distance. The Flash Lidar initiates its operation in an altimeter mode after the vehicle begins its braking phase and its altitude drops to about 20 km above the ground. In this mode of operation, the lidar transmitter laser is focused such that only a few of the detector array pixels are illuminated. This increases the operational range of the lidar from 1 km with all of its pixels illuminated to the 20 km with about 100 illuminated pixels. The altitude data is then provided to the flight computer to update the Inertial Measurement Unit (IMU) data and improve the vehicle position estimate from more than 1 km to about 300 m.

At about 15 km above the ground, the Flash Lidar will switch to the TRN mode by slightly increasing the transmitter beam divergence to illuminate about 200 pixels. In this mode, the Flash Lidar will continue to provide altitude data as well as generating consecutive 3-D images of the terrain with a lateral resolution of less than 6 m that is sufficient for performing the TRN function. The acquired images are correlated with stored on-board reference maps of known features such as craters and surface elevation data. The correlations are used to estimate the relative position error (map-tie error) between the surface and the inertial frames of the vehicle. Correlation of the Flash Lidar data with the surface elevation data obtained from prior orbiting laser altimeters are particularly reliable in estimating the map-tie error, thereby enabling the TRN algorithm to generate the trajectory correction needed for bringing the vehicle to within 30 m of the landing target.

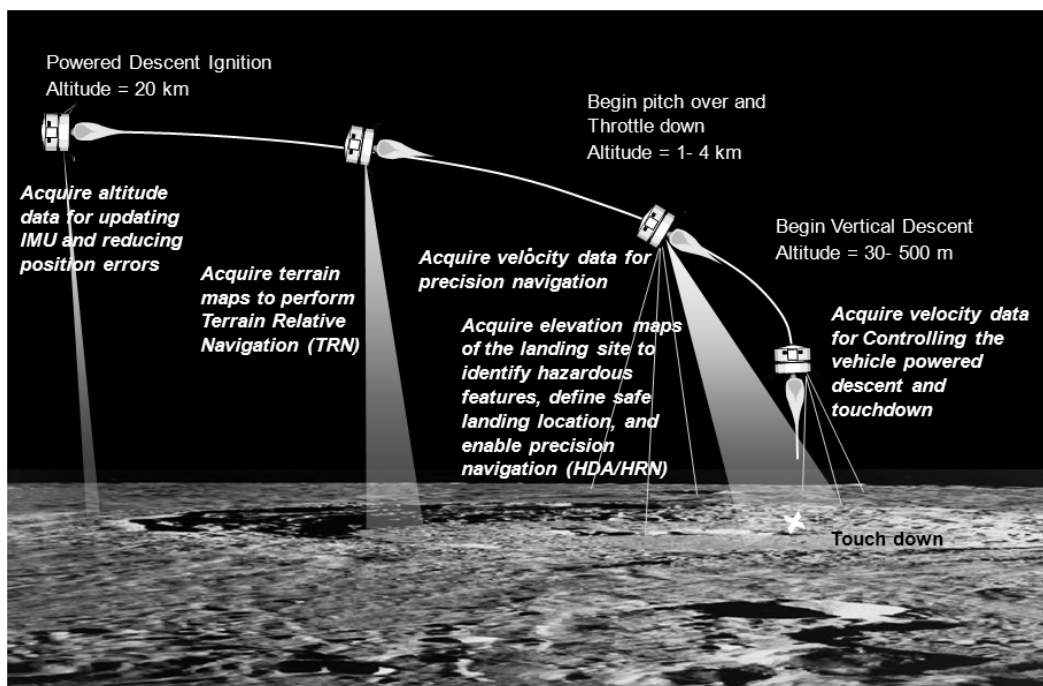


Figure 2. Operational scenario of landing sensors.

After completion of the TRN function at about 5 km above the ground, the lidar continues to provide altitude data so that the navigation error can be bounded. At about 1 km altitude, the laser beam divergence is increased to match the full field of view of the lidar receiver to begin its most critical function, which is hazard detection and avoidance/hazard

relative navigation (HDA/HRN). The HDA/HRN function requires detection of rocks and surface features greater than 30 cm in height, slopes greater than 5° over the diagonal of the footprint of the landing vehicle, and determination of position of landmarks to better than 1 m relative to the specified landing location (see Figure 3).

Various concepts for sensor operation and 3-D image acquisition are being evaluated. Each concept must provide the necessary information for achieving the ALHAT HDA/HRN performance goals and simultaneously provide situational awareness information. The primary metric for evaluating an operations concept is “robustness”, i.e. how efficiently, accurately, and reliably the job gets done. In the context of ALHAT this means that the operations concept must be fast, accurate, and be able to provide redundant information for real-time validation of the “decisions” or choices that it makes. All three of these descriptors are coupled in the sense that they all need to occur simultaneously for ALHAT to have credibility as a system.

A concept of operation, similar to “targeting”, that employs some of the capabilities being developed above, is termed as “intelligent” safe site selection using precision navigation. Here HDA/HRN have been coupled both in hardware and software since the process of determining hazard location is also the process for determining “landmarks” for relative navigation and can be done using the same sequence of 3-D images from the Flash Lidar. This mode of operation predicates on the concept that upon recognition of the first available “safe” landing site, the landing vehicle will be directed to it. Continuous operation of the Flash Lidar down to about 100 m above the ground will allow for high precision landing within the identified safe landing area, to about a meter of margin. The continuous operation of Flash Lidar at the video frame rate will also allow the determined “safe” location to be verified multiple times before the vehicle commits to touch down. To ensure that sufficient terrain area is monitored as the vehicle descends, an adjustable field-of-view (FOV) receiver optic is being considered. By increasing the receiver FOV according to its distance to the ground, the spatial coverage and resolution can be preserved.

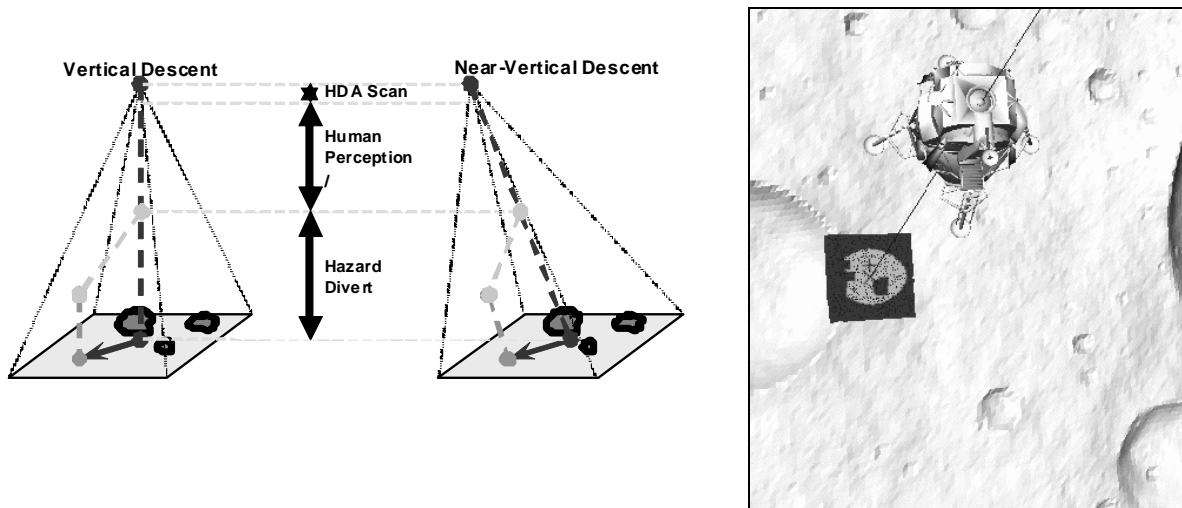


Figure 3. The hazard detection phase is expected to begin when the Lander pitches over to start its approach descent to the surface. The slope of descent can be adjusted to allow for sensor field of view considerations and, if necessary, for human interaction.

3. TESTING AND EVALUATION

The capabilities of the Flash Lidar technology for autonomous safe landing application have been investigated in a series of static and dynamic experiments at a sensor test range and from aircraft platforms. One of the major objectives of these tests was to define areas of technology improvement required to meet NASA’s autonomous safe landing needs. These tests also helped the development of various algorithms including image reconstruction, HDA, HRN, and TRN.

Furthermore, the analyses of the test data allow improvement to the Flash lidar computer models used in end-to-end landing system simulations. All the Flash Lidar experiments to date have been based on the technology developed by Advanced Scientific Concepts (ASC)^{4,5}. This 3-D Imaging camera has a 128x128 pixel array capable of generating real-time image frames at up to a 30 Hz rate. Characterization of Flash Lidars and other remote sensing instruments are routinely made at the long-range test facility at NASA-LaRC. Analyses of the ASC Flash Lidar test results from the long-range test facility at NASA-LaRC for specific landing applications have been reported previously⁶.

The ALHAT first airborne tests of the Flash Lidar system were conducted aboard an AS-350 helicopter to assess the technology's capabilities for terrain hazard detection. Figure 4 shows the ASC Flash lidar housed inside a gimbal that points on command to the desired area. The transmitter laser generated 13 mJ, 10 nsec pulses at an eye-safe wavelength of 1.57- μ m. The 3 degree FOV, f/2.2 receiver lens gave a 10 cm ground sample distance (GSD) from 250 m slant range. The helicopter flight tests were conducted above vegetation-free terrain at NASA Dryden Flight Research Center and Death Valley National Park in California. Hundreds of man-made rectangular and spherical targets with different reflectivity and varying sizes from 30 cm to several meters were placed and their locations registered (Figure 5). Several craters, each about 3 m in diameter and 1 m in depth, were also prepared for this test. Different flight patterns of up to 500 m over the ground were employed over the target areas. Figure 6 is an example of the lidar data showing targets on the ground. A detailed analysis of the helicopter test results can be found in a recent publication⁷.

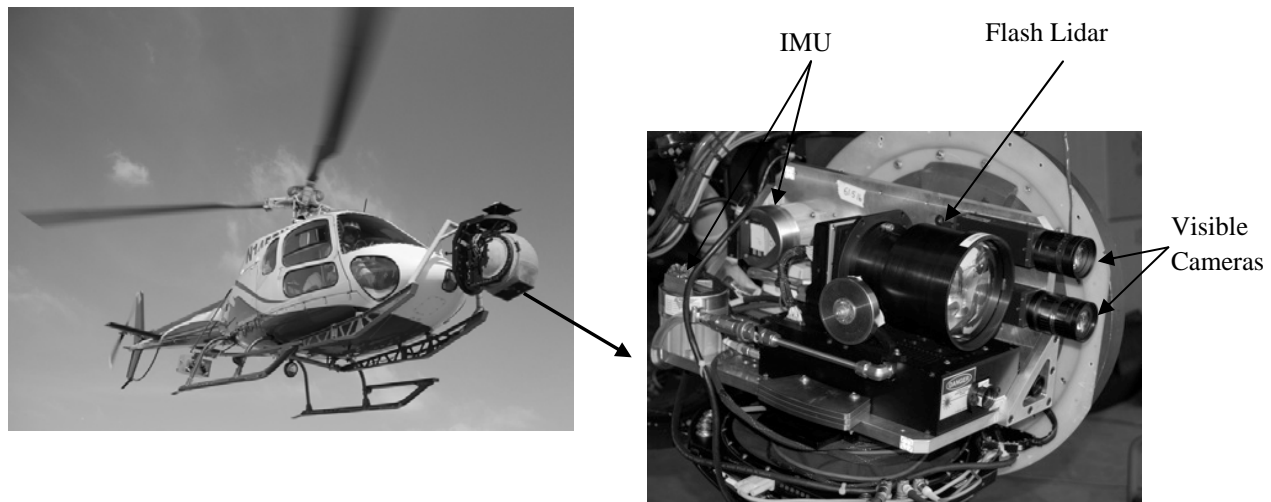


Figure 4. Flash Lidar mounted inside a gimbal for a series of helicopter flight tests.



Figure 5. Hundreds of rectangular and hemispherical targets with varying sizes from 30 cm to several meters placed at the test site and their location registered along with several man-made craters.

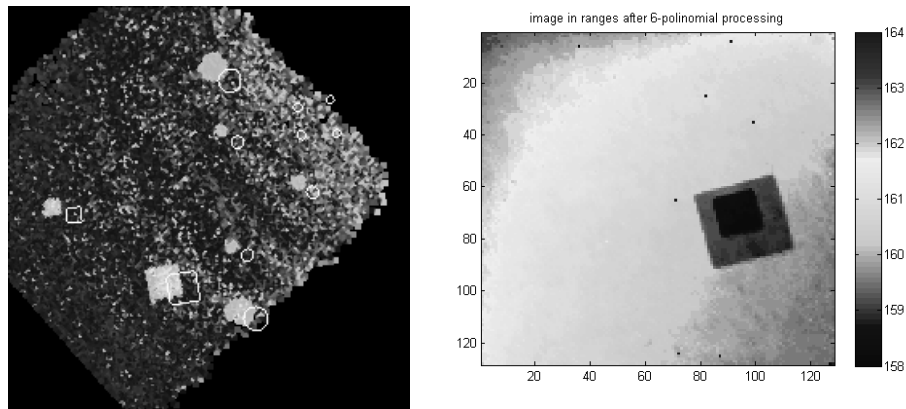


Figure 6. Examples of Flash Lidar image frames. Left image shows hemispherical and rectangular objects, and the right image shows two boxes with one on top of the other.

More recently, a similar flash lidar to the one used for the helicopter flight tests was integrated and flown onboard a fixed-wing aircraft to assess its performance for multiple pixel altimetry and terrain relative navigation functions. The Flash Lidar was mounted on a gimbal aboard a Beech King Air B200 aircraft, along with a laser altimeter, visible cameras, and an inertial measurement unit (IMU). Several flights were performed in areas of Death Valley and in the Nevada Test Site (NTS) with various flight profiles and altitudes reaching over eight kilometers above ground level. The Death Valley and NTS locations were selected primarily because of the topographical similarities to the lunar terrain. Figure 7 shows a mechanical drawing of the sensors mounted on the gimbal.

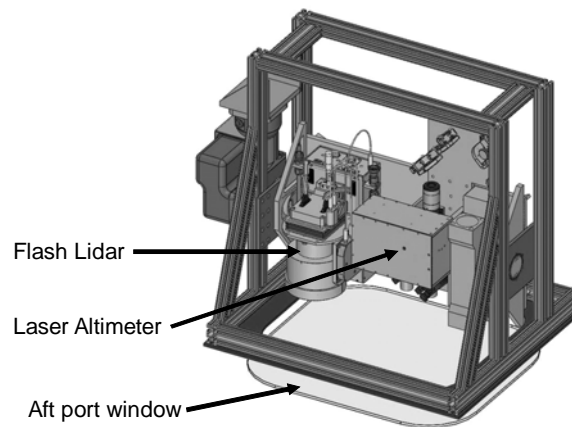


Figure 7. Flash Lidar and Laser altimeter configuration on gimbal onboard a King Air fixed-wing aircraft.

To operate at long line of sight (LOS) ranges, the Flash Lidar transmitter beam divergence was reduced, thus illuminating only a fraction of the FOV and a subset of the focal plane array (FPA) pixels. In this mode, the Flash Lidar has a much larger operational range than when the full FPA is illuminated. Although operational range is increased, the added concentration of energy on the illuminated pixels creates a gradient across the footprint of the beam on the ground that is greater than the gradient distribution obtained when the same laser beam illuminates the full FPA. Due to the

temporal response of the system to intensity⁶, this field test provides data that is used to investigate and mitigate this effect from the sensor for applications such as TRN. In preparation for this field test, the Flash Lidar system performance was well characterized at the Sensor Test Range⁶, and the sensor's operational range profile was predicted.

The transmitter beam divergence is chosen before the flight to maximize the number of active pixels for the upcoming altitude profile. Beam divergence was selected by changing the magnification of the transmitter beam expander to 1x (Bare Beam), 2x, 5x, or 10x. Table 2 below summarizes the flight missions and Flash Lidar transmitter configurations. Performance of the sensor during the shakeout flights and Flight 1 were used to estimate the correct beam divergence for all other flights.

Table 2. Aircraft Flight Test Campaign Summary.

Flight #	Area	Xmtr Optic	Altitude	Comment
Shakeout 1	NTS	5x	1- 8 km	No alt data, weather limited
Shakeout 2	NTS	2x	2 – 4.5 km	300-600 active pixels
Shakeout 3	NTS	2x	2 – 8 km	1400 count signals at 8 km
Flight 1	DV	5x	2 – 8 km	75-250 active pixels
Flight 2	DV	2x	~4 km	
Flight 3	DV	5x	8 km	
Flight 4				Cancelled
Flight 5	NTS	Bare Beam	2 – 4 km	200 – 1000 active pixels
Flight 6	NTS	10x	~8 km	No altimeter, diff. focus
Flight 7	NTS	2x	2-4 km	
Flight 8	DV	5x	~8 km	No altimeter, diff. focus

The comments listed in the table are selected highlights of each particular flight. For example, the number of active pixels listed corresponds to the resulting variations in number of triggered pixels from the lowest altitude to the highest altitude for that flight. The number of counts listed for Shakeout 3 highlights the fact that an average intensity of 1400 counts was obtained at the aircraft flight ceiling of approximately 8 km, using a 2x beam expander on the transmitter while flying over NTS. This data was used to select all future NTS flight configurations since detection threshold is 1000 counts. Figure 8 shows the average intensity per frame plotted against LOS range, data obtained from Flight 5. The humps in intensity are due to sections of higher ground reflectance as the “racetrack” profiles were flown.

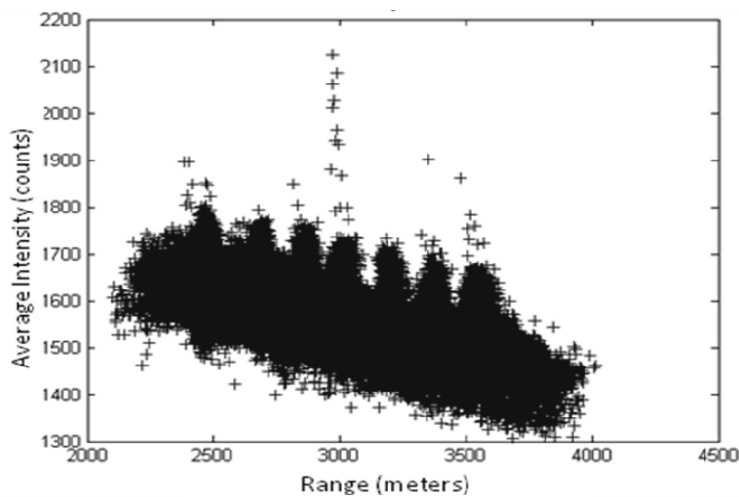


Figure 8. Average intensity in “counts” per frame vs LOS range.

Figure 9 shows the received intensity maps of four consecutive frames. The intensity units are in counts, corresponding to the digital dynamic range of the ROIC. The horizontal and vertical axes are pixels (128 x 128) of the FPA. At close inspection of these frames, one can recognize buildings moving across the FPA that are outside the illuminated pixels. These pixels are picking up background thermal radiation from the hot August Nevada sun. These images help the data analysis since the buildings were surveyed, and can provide range measurement truth to the 3-D reconstruction. The buildings also provide a quick look of the pulse-to-pulse area overlap of the beams on the ground. These images show that approximately 60% of the beam diameter overlaps from frame to frame. Although the beam divergence is fixed for each flight, the portion of the triggered pixels that overlap from frame to frame depends on frame rate, aircraft velocity, and signal to noise variables (SNR: altitude, atmospheric transmission, and ground reflectivity).

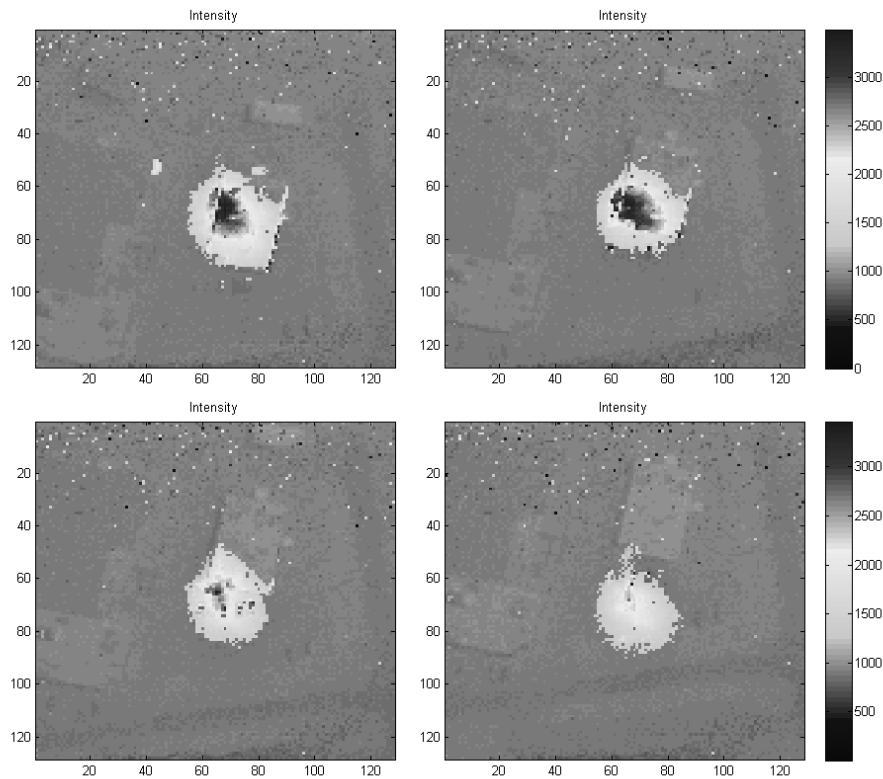


Figure 9. Intensity maps of four consecutive frames obtained during Flight 5.

The 3-D range map is shown in Figure 10 for the same 4 frames of Figure 9. The beam footprints displayed in Figure 9 show the gradients in the intensity distribution and Figure 10 shows how these nonlinear variations affect range measurement accuracy. Range correction algorithms are developed at NASA-LaRC based on controlled calibration experiments performed at the Sensor Test Range.

The long-range laser altimeter shared the gimbal with the Flash Lidar and measured the LOS range from a laser beam parallel to the Flash Lidar beam. This altimeter was developed in-house at NASA-LaRC in support of the ALHAT project. The altimeter has a low divergence transmitter and a narrow field of view receiver. The altimeter FOV is under one milliradian, and its beam footprint on the ground covers approximately four pixels of the Flash Lidar. The instrument has range measurement accuracy better than 20 centimeters. The altimeter serves to collect independent range measurements that can be used to compare against the multi-pixel ranges obtained from the Flash Lidar.

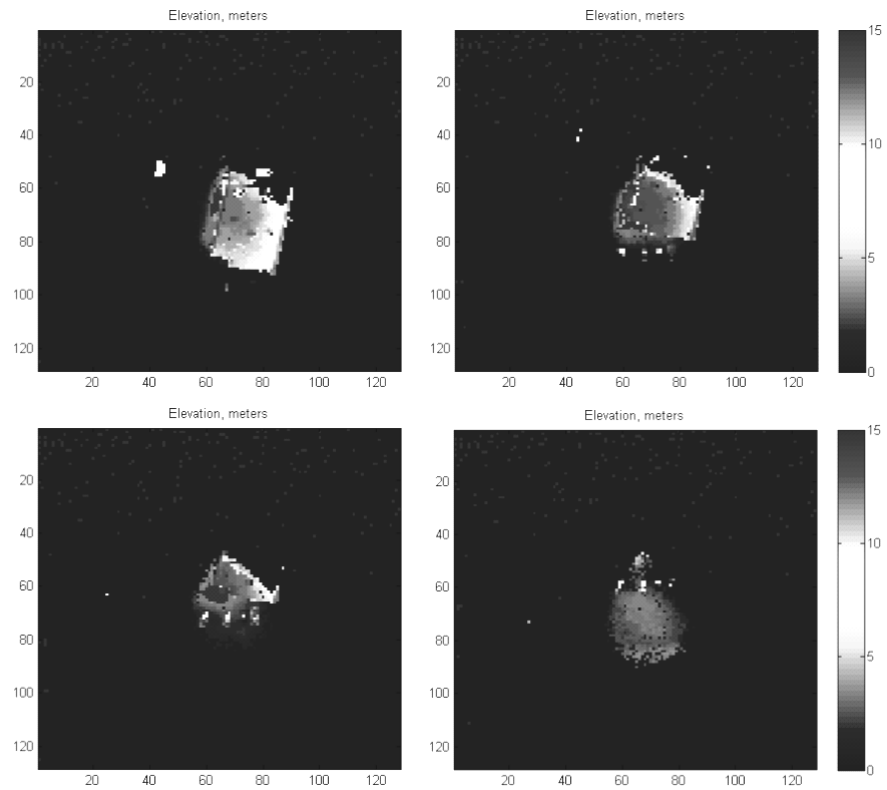


Figure 10. 3-D reconstruction of the same 4 frames shown in Figure 9.

Figure 11 shows a portion of Flight 5, comparing the laser altimeter to single pixel range measurements from the Flash Lidar. The difference in range between the two instruments is due to the geographical separation between the two laser beams on the ground. Performance of the Flash Lidar as a multi-pixel TRN instrument is under evaluation, and the results will be presented in future publications.

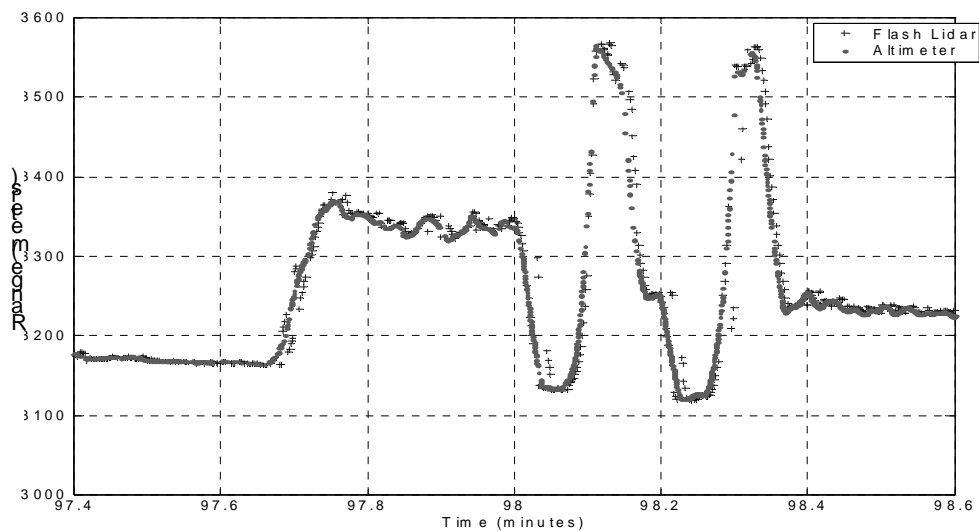


Figure 11. Laser altimeter compared to a single pixel range measurements.

4. FLASH LIDAR TECHNOLOGY ADVANCEMENT

The results of the static and airborne tests described above were proved critical in defining the areas of the technology improvement and development of signal processing algorithms necessary for achieving the ALHAT objectives and meeting NASA's autonomous safe landing needs. A series of Flash Lidar component technology advancement projects were initiated in 2008 in collaboration with industry, aimed at the development of a Flash Lidar landing sensor system that can efficiently perform the four functions described above. Table 3 summarizes the current state of the Flash Lidar technology and the performance goal of the current technology advancement activities.

Table 3. Flash Lidar ALHAT performance goals

Mode of Operation	Parameter	Current	Goal
HDA/HRN	Max operational range	400 m	> 1000 m
	Number of pixels	128X128	256X256
	FOV	3 deg	Variable 6 – 24 deg
	Precision	8 cm	5 cm
	GSD	20 cm	10 cm
	Map size	102 m X 102 m	204 m X 204 m
	Map acquisition time	1-2 sec	1 sec
TRN	Max operational range	8 km	20 km
	Number of illuminated pixels	10X10	20X20
	Precision	20 cm	20 cm
	Update rate	30 Hz	30 Hz

These activities include the development of low noise 256x256 pixel Avalanche Photodiode array, high sensitivity 256x256 Readout Integrated Circuit (ROIC), efficient transmitter laser with optimum pulse temporal and spatial profiles, programmable field-of-view receiver optics, and novel signal processing techniques. Increasing the number of pixels by a factor of 4 and extending the operational range of the lidar by a factor 2.5 translates to 25X more sensitive or more powerful system. This is expected to be achieved by increasing the detection sensitivity (i.e., combination of the detector array and ROIC performance) by 10X and by increasing the effective laser pulse energy by 2.5X. The generation of 3-D maps covering an area of the order of 200X200 meters with 10 cm resolution will be achieved by a combination of an advanced receiver optics design and novel signal processing techniques. A motorized optical mechanism is being developed to allow for increasing the lidar field of view as the vehicle descends thus preserving the coverage area during final approach phase. A set of signal processing algorithms are being developed for accurate calibration of the lidar signal and enhancing the image resolution and reducing its noise through "super resolution" or "digital magnification" techniques. Upon completion, these component technologies will be integrated into a system to demonstrate the Flash Lidar capabilities in meeting ALHAT's objectives.

5. CONCLUSION

The Flash Lidar has been identified by NASA as a key technology for enabling autonomous safe landing of future robotic and crewed lunar landing vehicles. The capabilities of Flash Lidar technology were evaluated through a series of static tests using a calibrated target and through dynamic tests aboard a helicopter and a fixed wing aircraft. The aircraft

flight tests were performed over Moon-like terrain in the California and Nevada deserts. These tests provided the necessary data for the development of signal processing software, and algorithms for hazard detection and navigation. The tests helped identify technology areas needing improvement and will also help guide future technology advancement activities. The Flash Lidar component technologies being developed under the ALHAT project will be integrated into a system capable of generating 3-D image frames with 256x256 pixels resolutions from 1 km distance at 30 Hz rate meeting the specified goals for future landing vehicles.

ACKNOWLEDGMENTS

The authors would like to acknowledge ALHAT project manager, Chirold Epp, NASA Johnson Space Center for his invaluable support. The authors are thankful to the contributions of NASA Jet Propulsion Laboratory ALHAT team for facilitating the aircraft flight tests campaigns. The authors are also thankful to Advanced Scientific Concepts for providing the Flash lidar systems and supporting the static and airborne tests.

REFERENCES

- [1] Epp, C.D., Robinson, E.A., and Brady, T., "Autonomous Landing and Hazard Avoidance Technology (ALHAT)", Proc. of IEEE Aerospace Conference, pp.1-7 (2008).
- [2] Amzajerjian, F., Pierrottet, D., Tolson, R. H., Powell, R. W., John B. Davidson, and Peri, F., "Development of a Coherent Lidar for Aiding Precision Soft Landing on Planetary Bodies," Proc. of 13th Coherent Laser Radar Conference, Kamakura, Japan (2005).
- [3] Pierrottet, D., Amzajerjian, F., Petway, L., Barnes, B., and Lockard, G., "Flight test performance of a high precision navigation Doppler lidar," Proc. SPIE, Vol. 7323 (2009).
- [4] Stettner, R., Bailey, H., and Richmond R., "Eye Safe Laser Radar Focal Plane Array for Three-Dimensional Imaging", Proc. of the SPIE Vol. 4377 (2001).
- [5] Stettner, R., Bailey, H., and Silverman S., "Three Dimensional Flash Ladar Focal Planes and Time Dependent Imaging," International Symposium on Spectral Sensing Research, Bar Harbor, Maine (2006).
- [6] Pierrottet, D., Amzajerjian, F., Meadows, B., Estes, R., Noe, A., "Characterization of 3-D imaging lidar for hazard avoidance and autonomous landing on the Moon," Proc. of SPIE Vol. 6550 (2007).
- [7] Bulyshev, A., Pierrottet, D., Amzajerjian, F., Busch, G., Vanek, M., and Reisse, R., "Processing of three-dimensional flash lidar terrain images generating from an airborne platform," Proc. SPIE, Vol. 7329 (2009).